

Online-growth measurements on the generation of metal nanoaerosol and their offline structural properties

Shubhra Kala^{a*}, B R Mehta^b & F E Kruis^c

^aDepartment of Physics, H.N.B. Garhwal University, Srinagar (Garhwal) 246 174, India

^bThin Film Laboratory, Department of Physics, Indian Institute of Technology Delhi 110 016, India

^cInstitute for Nanostructures and Technology, Faculty of Engineering Science, University of Duisburg-Essen, Duisburg 47057, Germany

Received 31 January 2020

Aerosol, which is intentionally generated in the laboratory, is utilized to synthesize nanoparticles. As the size of suspended nanoparticles in nano regime, therefore, purposely generated aerosol is termed as nanoaerosol. The present study demonstrates the formation metal nanoparticles in gas-phase. For this purpose, the initial condition; is to create nanoaerosol that is, suspension of tiny metal particles in gas. By evaporating a metal source in the presence of gas, creates the condition of supersaturation and then by nucleation and condensation forms stable nuclei, which grow in size to form primary particles in gas. A high-temperature furnace is utilized to evaporate metal e.g. palladium with 10% silver (PdAg), in the high purity nitrogen, is known as a carrier gas. During the sparking process, growth of the PdAg nanoaerosol is monitored online by a scanning mobility particle sizer, as a function of different parameters. Size-distribution in produced nanoaerosol shifts towards larger mobility equivalent diameter value from 7.83 to 42.6 nm along-with the increase in number concentration, on increasing the evaporation temperature from 1200 to 1400 °C. To study the effect of sintering temperature on particle size, size-fractionation by a differential mobility analyzer and in-flight sintering of PdAg nanoaerosol have been carried out. On increasing the sintering temperature, the size of selected PdAg nanoparticles reduces. The geometric mean mobility equivalent diameters of fractionated PdAg nanoparticles of 17.9, 25.3 and 30.9 nm reduces to 15.2, 19.4 and 21.7 nm, respectively, due to the compaction. The value of geometric standard deviation is approximately 1.10, which reflects the monodisperse nature of PdAg nanoparticles in the generated nanoaerosol. An electrostatic precipitation technique is utilized to separate out PdAg nanoparticles from nanoaerosol onto suitable substrates. Formation of spherical and mono-crystalline PdAg nanoparticles is revealed by TEM studies.

Keywords: Nanoparticles, Aerosol, PdAg alloy

1 Introduction

The ability to vary nanoparticle size over a wide range with an accurate control of size-distribution, well-defined shape and without varying the surface structure are the important requirements for a synthesize method to qualify as a useful nanotechnological tool for realizing size-dependent properties and tailoring these for specific applications. Palladium (Pd) has been extensively investigated due to its novel catalytic properties. Pd is used as a hydrogen catalyst in many industrial applications. Due to high diffusion of H in Pd and its high sticking coefficient, Pd is also a useful material for hydrogen sensing. Enhanced surface area at nano dimensions and structural and electronic modifications due to nanoparticle size has resulted in Pd nanoparticles to be more useful in various applications¹. A variety of

synthesis methods based on chemical, electrochemical, reverse micelles, sonochemical and pulsed laser ablation processes been used for growing Pd nanoparticles²⁻⁷. In order to improve hydrogenation properties of Pd nanoparticles, alloying with Ag, Au, Pt and Ni has been tried. Submicron Ag–Pd alloy particles were reported to synthesize by spray pyrolysis⁸. The liquid flame spray, a high temperature aerosol method, has been used to generate Ag–Pd alloy nanoparticles from Ag and Pd nitrate precursors⁹. Although, Pd nanoparticles in pure and alloyed form show useful properties there has been less effort towards preparing Pd nanoparticle having different size range and with controlled size-distribution. Synthesize of nanoparticles of larger size with narrow size distribution and monocrystalline nature is difficult due to two reasons. First, nanoparticles of larger sizes require larger growth at higher temperatures. Second, sintering of larger sized nanoparticles has to be carried out for longer time

*Corresponding author (E-mail: shubkala@gmail.com)

or at high temperature. These are the conditions of higher agglomeration. In the present study, gas phase synthesis of PdAg nanoparticles by evaporation in conjunction with size-selection using a differential mobility analyzer has been carried out. In-flight sintering of the nanoparticles results in PdAg nanoparticle having mono-crystalline nature and quasi spherical shape along-with well-defined size-distribution in a larger size range of 15-25 nm.

2 Experimental Details

2.1 Methodology

The basic steps used to prepare size-selected Pd nanoparticles the gas-phase technique are summarized below¹⁰;

- (i) Production of vapor species of PdAg in a free flowing N₂ carrier gas, which subsequently converted into primary particles by nucleation and condensation and finally to agglomerates of different sizes as a result of coagulation.

- (ii) Electrical mobility based fractionation of PdAg agglomerates by means of a differential mobility analyzer. Electrical mobility depends on the shape, size and charge level of particles/agglomerates.
- (iii) Compaction and crystalline of Pd agglomerates during their flight in carrier gas.
- (iv) The mechanism of nanoparticles formation by the gas-phase technique^{11, 12} is schematically represented in Fig.1

2.2 Process setup

Experimental setup, schematically shown in Fig. 2, is consists of an evaporation tube furnace inside which PdAg granules are placed in a ceramic crucible. A provision is made to enter carrier gas inside the tube through mass flow controller. After that a ultra-violet charger, a homemade radial differential mobility analyzer (DMA), a sintering furnace and an electrostatic precipitator (ESP) are connected in series. On increasing the temperature of evaporation

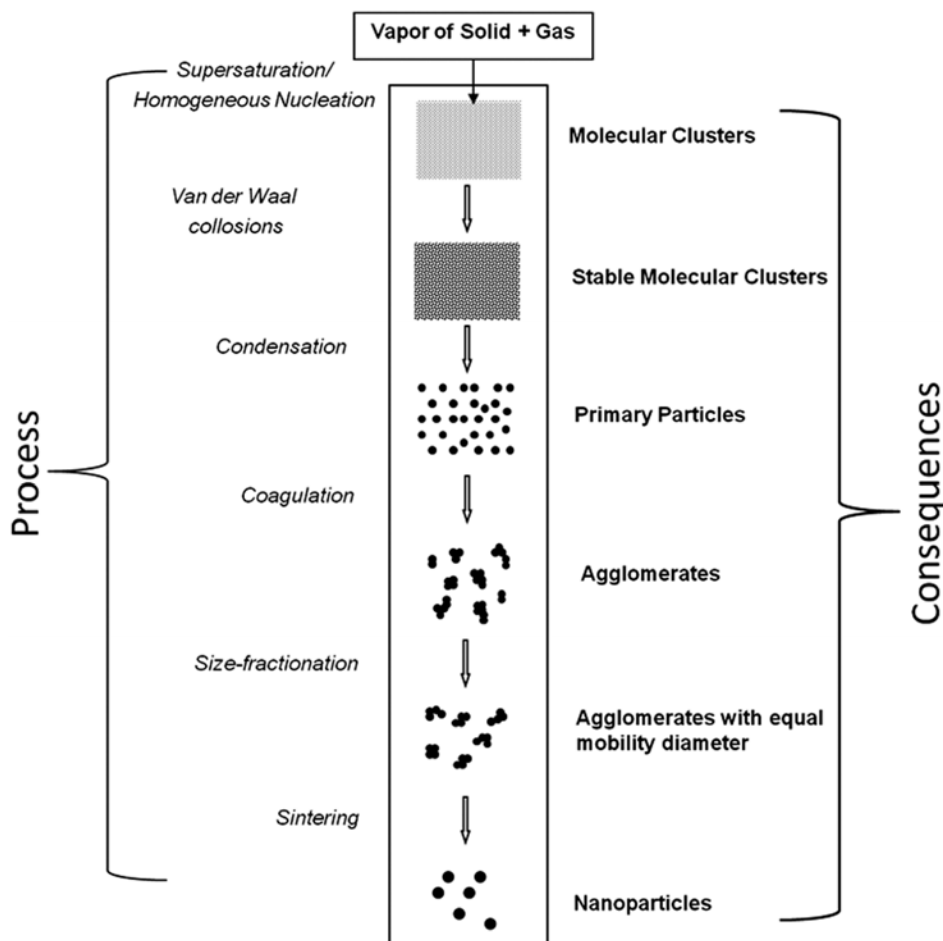


Fig. 1 — Schematic representation of different steps of nanoparticle formation in gas-phase.

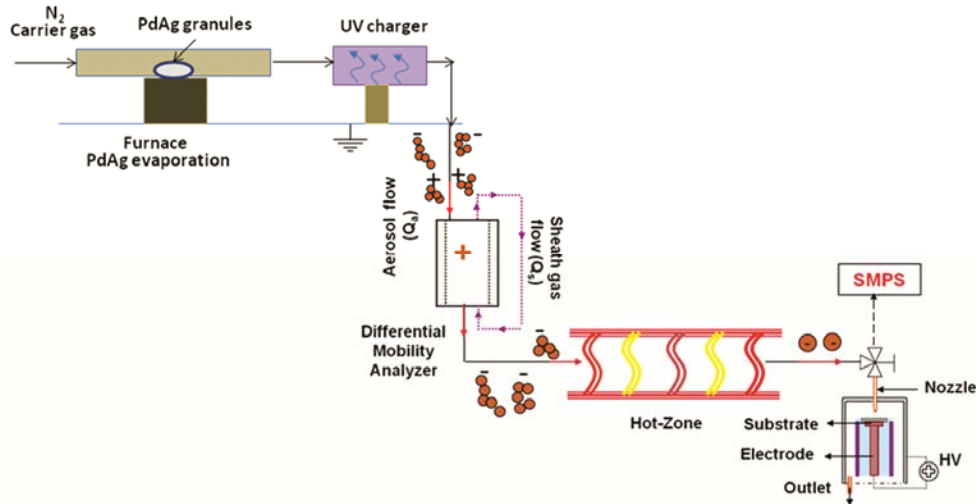


Fig. 2 — Schematic of experimental setup, a combination of an evaporation furnace, a UV charger, a differential mobility analyzer, a sintering furnace and an electrostatic precipitator (ESP).

furnace, PdAg material evaporates in the presence of carrier gas. Vapors of PdAg cool down rapidly as it moves away from the heating zone which leads to supersaturation and hence, formation of primary particles due to nucleation and condensation. On moving along-with the carrier gas, primary particle coagulate to form bigger particles. The suspension of particles of different sizes in carrier gas is called as polydisperse aerosol. Thus, generated polydisperse aerosol then enters the UV charger, where particles gain the charges and then enters into DMA where, polydisperse aerosol undergoes size-fractionation. DMA classifies particles/agglomerates on the basis of electrical mobility equivalent diameter (D_m) which takes into account the charge level, the mass and the shape of the particles/agglomerates. During size classification, the resolution of size-distribution depends upon the aerosol to sheath gas flow rate ratio within the DMA. During size fractionation, polydisperse aerosol to sheath gas ratio ($Q_a: Q_{sh}$) is kept 1:10. An online technique, scanning mobility particle sizer (SMPS) is utilized to study the effect of evaporation temperatures on size-distribution and concentration of generated particles. The size-fractionated aerosol i.e., monodisperse is then allowed to pass through hot zone (furnace) in order to convert suspended particles into spherical and crystalline particles. Then from monodisperse aerosol, the nanoparticles are removed and collected onto Cu grids by electrostatic precipitation (ESP) technique. In ESP, high voltage in the range 2-5 keV (depending on the substrate) is applied between the central electrode and walls of ESP (electrically grounded) to focus the

aerosol flow. Substrate is kept on the center electrode of ESP, perpendicular to the flow of aerosol at a distance of 5 mm from the entrance nozzle. Monodisperse nanoaerosol on entering ESP through the nozzle expands and suffers retardation in the velocity. Due to the combined effect of the retardation in the velocity and the applied electric field, particles move towards the substrate and get deposited.

In the present study, scanning mobility particle sizer (SMPS) is used to measure online particle size-distribution, at different stages of growth. A SMPS comprises of an electrostatic classifier and an ultrafine condensation particle counter. An electrostatic classifier consists of an impactor, a Kr-85 bipolar charger, a sheath-air flow controller, a high-voltage controller and a DMA. The Electrostatic classifier initially removes particles above a known particle size by inertial impaction. Then aerosol particles acquire charge with a well known Boltzmann charge distribution¹³ by neutralizer, which bombards the bipolar ions. An ultrafine condensation particle counter is an optical counter, which calculates particles number concentration after making particles sufficiently enlarged by a condensing vapor.

3 Results and Discussion

By maintaining continuous carrier gas flow of 2.0 slm (standard litre/min) inside the furnace fixed, evaporation temperature is increased from 1000 to 1400 °C. With the increasing the evaporation temperature, particle size-distribution shifts towards the larger mobility diameter (D_m) value and also particle number concentration increases, as shown in

Fig. 3 (a). As substantial particle count is observed at temperatures above than 1200 °C, therefore, particles size-distributions are considered at temperatures ≥ 1200 °C. The geometric mean mobility diameter (D_{gm}) increases from 7.83 to 42.6 nm on increasing the evaporation temperature 1200 to 1400°C, as shown in Fig. 3(b). Particle number concentration increases from 3.71×10^6 to 5.42×10^7 cm^{-3} as evaporation temperatures increases from 1200 to 1400°C (Fig. 3(c)). With the increase in the evaporation temperature, relatively more PdAg mass evaporates per unit volume of the carrier gas, results in higher supersaturation and formation of larger number of primary particle. The coagulation tendency between the primary particles depends upon the number concentration. So higher concentration of primary particles at higher evaporation temperature results in enhance coagulation and hence formation of agglomerates of larger size. Thus, particle size distribution of produced PdAg agglomerates shifts towards larger average D_{gm} value along-with the increase in number concentration on increasing

the temperature. Figure 3(d) shows bright field transmission electron microscopic (TEM) image of PdAg agglomerates produced at evaporation temperature 1400 °C with carrier gas flow of 2.0 slm. As clear from the image that the PdAg particles are irregular shaped agglomerates, having chain-like structures and consisting of small primary particles of sizes 2-4 nm. Normally, primary particle size by phase technique is reported between 3.5- 5.0 nm^{13,14}.

Three different sized PdAg agglomerates of D_{gm} values of 18.0 nm (PA1), 25.3 nm (PA2) and 30.9 nm (PA3) are selected by applying positive voltages of 0.6, 1.2 and 1.8 kV, respectively, to the DMA . As mentioned before, the agglomerates are open fractal like structures, hence in order to convert them into spherical particles sintering is essential. Therefore, these classified agglomerates are afterwards subjected to sintering during their flight between DMA and ESP. Effect of sintering on agglomerates is studied in the temperature range from 30 to 950 °C, by online measurement using

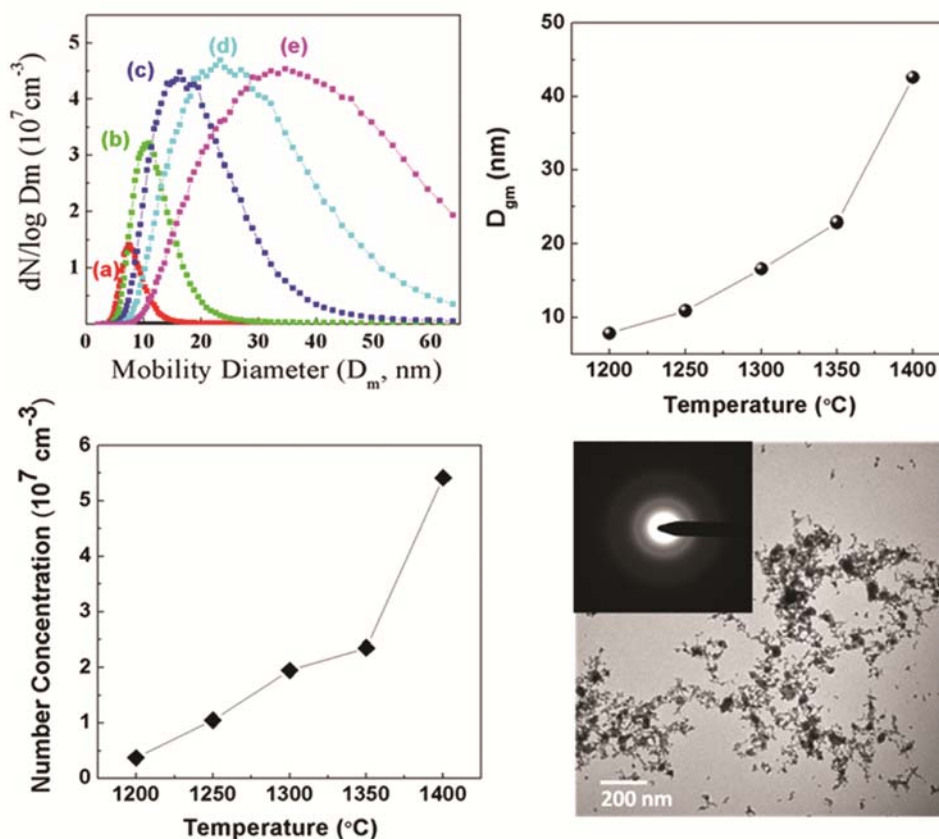


Fig. 3 — (a) Size-distribution of PdAg agglomerates produced at different temperatures (a) 1200 °C, (b) 1250 °C, (c) 1300 °C, (d) 1350 °C and (e) 1400°C. (b) Geometric mean mobility diameter, (c) total number concentrations at mentioned temperatures and (d) bright field TEM micrograph and selected-area diffraction pattern of polydisperse PdAg agglomerates.

a SMPS. Reduction in D_{gm} value is observed on increasing the sintering from 30 to 950 °C, as shown in fig. 4(i). This decrease in the D_{gm} value is normally related to restructuring and compaction of agglomerates, which occurs during sintering. For all the three selected agglomerates, D_{gm} value vs sintering temperature plots follow the similar trends, as clear from the Fig. 4(a). In the beginning, D_{gm} value decreases rapidly, after that almost remains constant and then again decreases slowly with the increase in sintering temperature. The initial rapid shrinkage in D_{gm} value is due to the restructuring and compaction of the agglomerates during sintering. The nearly constant region indicates that compaction of the agglomerates is complete. A further decrease in D_{gm} value indicates partial evaporation of materials from the surface of particles¹³. Figure 4 (b-d) shows the size-distributions of the samples PA1, PA2 and PA3 before and at sintering temperatures 200 °C, 400 °C, 600 °C, 800 °C and 950 °C. Without applying sintering the size-distribution is denoted by RT. As

clear from the figures that on increasing sintering temperature, along-with decrease in D_{gm} value, particle number concentration also diminishes. This reduction in particle number concentration is attributed to the temperature gradient inside the sintering furnace, which increases with the increase in the sintering temperature. In all the samples, the two size distributions are observed at 950 °C. The appearance two size-distributions indicate the partial evaporation of the particle during sintering. Therefore, sintering was performed only up to 800 °C. After sintering at 800 °C, measured D_{gm} values for the samples PA1, PA2 and PA3 by SMPS are 15.2 nm, 19.4 nm and 21.7 nm, respectively. TEM micrographs of the sample PA1 after sintering at 400, 600 and 800 °C are shown in Fig. 5. The TEM micrograph obtained after sintering 800°C, clearly shows that the deposited particles are quasi-spherical in shape. The sharp rings in the selected area electron diffraction pattern, as shown in inset, reveals the crystalline nature of the prepared PdAg nanoparticles.

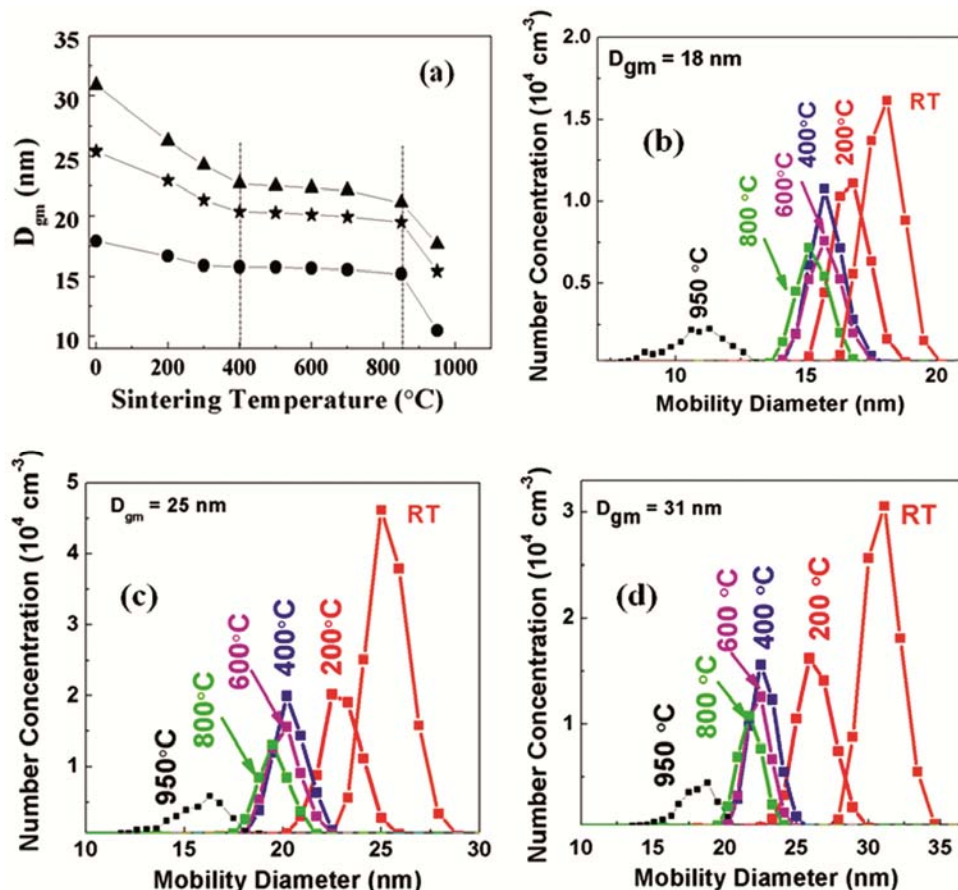


Fig. 4 — Effect of sintering temperature on the fractionated particles of D_{gm} values 18, 25 and 29 nm. Size-distributions of the fractionated particles of D_{gm} values (a) 18 nm, (b) 25 nm and (c) 31 nm at different temperatures. RT denoted room temperature.

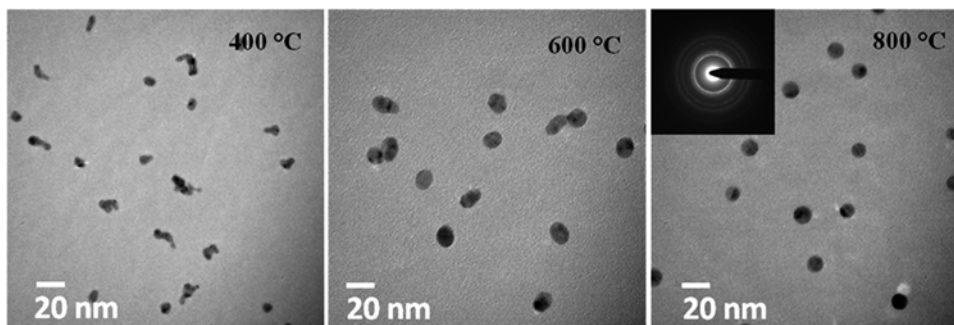


Fig. 5 — TEM images of PdAg nanoparticles, obtained after subjecting sintering 400, 600 and 800 °C. Inset shows the SAED pattern of the PdAg nanoparticles after sintering at 800 °C.

4 Conclusions

Present paper demonstrates a technique to produce nanoparticles of metals in gas-phase by taking PdAg alloys as an example. Significance of all synthesis steps are enumerated as well as demonstrated. Ability to produce specific sized nanoparticles with well-defined distribution is the key features of the present technique. Continuous online monitoring of nanoparticles during synthesis enables the possibility to manipulate the synthesis process, as per requirements.

Acknowledgement

Authors gratefully acknowledge the financial support of the DFG in the framework of SFB-445 “Nanoparticles from the gas phase: Formation, structure and properties”.

References

- 1 Khanuja M, Kala S, Mehta B R & Kruis F E, *Nanotechnology*, 20 (2009) 015502.
- 2 Zhang P & Sham T K, *Appl Phys Lett*, 82 (2003) 1778.
- 3 Teranishi T & Miyake M, *Chem Mater*, 10 (1998) 594.
- 4 Speets E A, Dordi B, Ravoo B J, Oncel N, Hallbäck A S, Zandvliet H J W, Poelsema B, Rijnders G, Blank D H V & Reinhoudt D N, *Small*, 4 (2005) 395.
- 5 Allmond C E, Oleshko V P, Howe J M & Fitz-Gerald J M, *Appl Phys A*, 82 (2006) 675.
- 6 Cho J K, Najman R, Dean T W, Ichihara O, Muller C & Bradley M, *J Am Chem Soc*, 128 (2006) 6276.
- 7 Das N A & Gedanken A, *J Mater Chem*, 8 (1998) 445.
- 8 Pluym C T, Kudas T T, Wang L M & Glicksman H D, *J Mater Res*, 10 (1995) 1661.
- 9 Keskinen H, Maˆkela J M, Vippola M, Nurminen M, Liimatainen J, Lepisto T & Keskinen J, *J Mater Res*, 19 (2004) 1544.
- 10 Kruis F E, Maisels A, Weber T & Hontanon E, *J Nanosci Nanotechnol*, 7 (2007) 1703.
- 11 Swihart M T, *Curr Opin Colloid Interf Sci*, 8 (2003) 127.
- 12 Roth P, *Proc Combustion Institute*, 31 (2007) 1773.
- 13 Kala S, Mehta B R & Kruis F E, *Rev Sci Instr*, 79 (2008) 013902.
- 14 Kala S, Mehta B R, Singh V N & Kruis F E, *J Mater Res*, 24 (2009) 2276.